

Thermal Effects on Photon-Induced Quantum Transport in a Single Quantum Dot

M. O. Assunção, E. J. R. de Oliveira, J. M. Villas-Bôas, and F. M. Souza
Instituto de Física, Universidade Federal de Uberlândia, 38400-902, Uberlândia, MG, Brazil
(Date: November 26, 2018)

We theoretically investigate laser induced quantum transport in a single quantum dot attached to electric contacts. Our approach, based on nonequilibrium Green function technique, allows to include thermal effects on the photon-induced quantum transport and excitonic dynamics, enabling the study of non-Markovian effects. By solving a set of coupled integrodifferential equations, involving correlation and propagator functions, we obtain the photocurrent and the dot occupation as a function of time. Two distinct sources of decoherence, namely, incoherent tunneling and thermal fluctuations, are observed in the Rabi oscillations. As temperature increases a thermally activated Pauli blockade results in a suppression of these oscillations. Additionally, the interplay between photon and thermal induced electron populations results in a switch of the current sign as time evolves and its stationary value can be maximized by tuning the laser intensity.

I. INTRODUCTION

Quantum transport in semiconductor quantum dots and molecular systems is a subject of intense study nowadays.¹ These nanoscaled devices provide a formidable environment to study fundamental aspects of quantum physics, involving many-body correlations and light-matter interaction in regimes out of equilibrium.² These systems have a great potential to form a new generation of optoelectronic devices based on the unique electronic structure that arises from the quantum confinement. For instance, quantum dots can produce a wealth of visible colors depending upon its size, even white light with relatively high efficiency³ and potential to integrability with nanoelectronics.⁴ Additionally, with the great technological advances in the manufacturing of semiconductor quantum dot system, it became possible to coherent monitor and control electron populations in two-level systems via different pump-probe techniques.⁵⁻⁸ In all these experiments the main signature of quantum coherent nonlinearity is Rabi oscillations, which has no classical counterpart. More recently, Rabi oscillations was also reported in organic light-emitting diode.⁹ Such coherent optical manipulations constitute a fundamental ingredient to quantum information processing in solid state devices that use electron-spin or excitonic states as qubits.¹⁰ Interestingly, holes in semiconductor quantum dots have been revealed as an alternative to electrons in the manufacturing of spin qubits.¹¹

It was originally demonstrated by Zrenner *et al.*¹² that coherent Rabi oscillations in a two-level quantum dot photodiode can be monitored by photocurrents. Additionally, it was proposed that a photocurrent in a self-assembled quantum dot photodiode can become spin-polarized due to an effective exchange interaction via biexciton state.¹³ This result points out the potentiality of the present system to future spintronic devices. It was also observed that the double dot structures present the ability to increase the coherence time of indirect excitons.¹⁴ Recently, thermal effects on the excitonic Rabi rotations in a quantum dot system were investigated experimentally.^{15,16} It was evidenced acoustic phonons as

the main source of damping of the Rabi oscillations.

In the present work we analyze how the temperature of nearby contacts tunnel coupled to a single quantum dot affects the coherent optical dynamics. Applying nonequilibrium Green function technique to a microscopic Hamiltonian model, we write a set of coupled integrodifferential equations that describes the coherent evolution of the electron-hole populations in the dot, enabling the study of non-Markovian effects. A resonant laser field drives the electron-hole dynamics and generates a photocurrent. We find two contributions to the current. The first one comes from electrons in the dot that tunnel to a contact. This current is positive and is mainly induced by the laser field. The second current component is related to electrons in the reservoir that acquires enough thermal energy to tunnel into the dot. This second contribution charges the dot, thus generating additional features not yet reported in the literature. Our main findings include the suppression of the Rabi oscillation as the temperature of the nearby contact increases, a negative photocurrent due to a backwards charge flow, and a maximum photocurrent value achieved when the laser intensity is comparable to the mismatch between the excited dot level and the contact chemical potential. Moreover, we analyze how the initial electron population of the conduction band, which is controlled by the temperature, affects the Rabi oscillations.

II. MODEL AND FORMULATION

Figure (1) illustrates the system considered. It is composed of a quantum dot attached to a left and to a right electron reservoirs in the presence of a source-drain bias voltage. A laser field shines the dot, thus generating electron-hole pairs in it. The electrons in the conduction band and the holes in the valence band can tunnel out from the quantum dot to the left and to the right reservoirs, respectively. This results in a photocurrent signal in the system. In the experimental point of view this system can be implemented in a structure of the kind n-GaAs-i-Schottky contact, as described in Ref.[12]. Al-

ternatively, a p - i - n junction can also be applied as describe in Ref.[17], with self-assembled quantum dots in the intrinsic region.

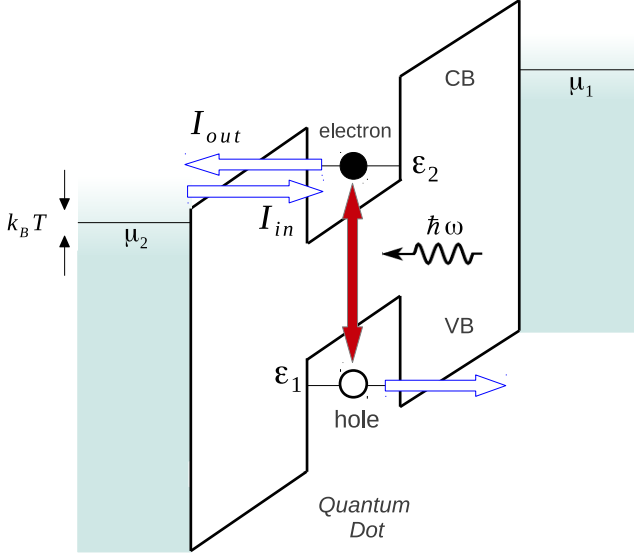


FIG. 1. (Color online) Sketch of the system studied. A quantum dot is tunnel coupled to both left and right reservoirs. The left reservoir illustrated has chemical potential μ_2 and temperature T . Due to the proximity of the conduction band level ϵ_2 to μ_2 , the dot population thermally fluctuates. This induces nonlinearities in the photocurrent driven by a laser field with resonant energy $\hbar\omega$.

The modeling Hamiltonian is given (per spin) by $H_\sigma = H_{D,\sigma} + H_{T,\sigma} + H_{L,\sigma} + H_{R,\sigma}$, with

$$H_{D,\sigma} = \sum_i \epsilon_{i\sigma} d_{i\sigma}^\dagger d_{i\sigma} + \gamma e^{-i\omega t} d_{2\sigma}^\dagger d_{1\sigma} + \gamma^* e^{i\omega t} d_{1\sigma}^\dagger d_{2\sigma}, \quad (1)$$

where $\epsilon_{i\sigma}$ is the dot level for spin σ in the valence ($i = 1$) or the conduction ($i = 2$) band. The operators $d_{i\sigma}$ ($d_{i\sigma}^\dagger$) annihilates (creates) one electron in level i with spin σ . The parameter γ gives the optical transition between valence band and conduction band in the quantum dot. This parameter can be controlled by the intensity of the incident radiation. In our model electron-electron interaction is not accounted for in order to allow analytical treatment. To couple the dot to fermionic reservoirs we use the tunneling Hamiltonian

$$H_{T,\sigma} = \sum_i \sum_{k_i} (t_i c_{k_i\sigma}^\dagger d_{i\sigma} + t_i^* d_{i\sigma}^\dagger c_{k_i\sigma}), \quad (2)$$

where $c_{k_i\sigma}$ ($c_{k_i\sigma}^\dagger$) annihilates (creates) one electron in the right ($i = 1$) or the left ($i = 2$) lead.¹⁸ The parameter t_i gives the dot-leads coupling strength. Finally, the free-electron energies of the electrons in both leads are given

by

$$H_{L,\sigma} + H_{R,\sigma} = \sum_{i=1}^2 \sum_{k_i} \epsilon_{k_i\sigma} c_{k_i\sigma}^\dagger c_{k_i\sigma}. \quad (3)$$

In the present model we assume that the tunneling rates are larger than spontaneous emission rates, so that electron-hole recombination will be neglected.

Our main task is to explore the effects of the reservoirs temperature on the Rabi oscillations and the photocurrent. To this goal we must find the lesser and retarded Green functions of the quantum dot, i.e., $G_{ij\sigma}^<(t, t) = i \langle d_{j\sigma}^\dagger(t) d_{i\sigma}(t) \rangle$ and $G_{ij\sigma}^r(t, t') = -i \theta(t - t') \langle \{ d_{i\sigma}(t), d_{j\sigma}(t') \} \rangle$. Note that the occupations of the levels $\epsilon_{i\sigma}$ are given by $n_{i\sigma}(t) = \text{Im} \{ G_{ii\sigma}^<(t, t) \}$, while the photocurrent is defined as $I_{i\sigma} = -e \langle \dot{N}_{i\sigma} \rangle = -e i \langle [H_\sigma, N_{i\sigma}] \rangle$, ($\hbar = 1$) with $N_{i\sigma} = \sum_{k_i} c_{k_i\sigma}^\dagger c_{k_i\sigma}$ being the total number of particles operator. Following Ref. [2] one can show that

$$I_{2\sigma}(t) = -e \Gamma_{2\sigma} n_{i\sigma}(t) + 2e \text{Re} \{ \Phi_{22\sigma}^r \} \quad (4)$$

where $\Phi_{22\sigma}^r(t) = \int_{-\infty}^t dt_1 G_{22\sigma}^r(t, t_1) \phi_{2\sigma}(t_1, t)$ and

$$\phi_{i\sigma}(t_1, t) = i \Gamma_{i\sigma} \int \frac{d\epsilon}{2\pi} f_i(\epsilon) e^{-i\epsilon(t_1 - t)}, \quad (5)$$

with $i = 1, 2$. Here $f_i(\epsilon)$ is the Fermi function to i -th reservoir and $\Gamma_{i\sigma} = 2\pi |t_i|^2 \rho_{i\sigma}$ is the tunneling rate with $\rho_{i\sigma}$ being the density of states of the corresponding reservoir for spin component σ . The present formalism allows the inclusion of ferromagnetic leads by considering spin-dependent tunneling rates $\Gamma_{i\sigma}$.¹⁹ According to Eq. (4) the current at time t has two contributions, one that is instantaneous and proportional to the dot occupation $n_{i\sigma}(t)$ (I_{out}) and a second one that involves the whole history of the system (I_{in}). In this second term, a time integral of the correlation function $G_{22\sigma}^r(t, t_1)$ weighted by a thermal dependent function $\phi_{2\sigma}(t_1, t)$ should be carried on, ranging from $-\infty$ to the present time. All the thermal effects arise via this memory integral. This contrasts to the density matrix approach used in quantum optics formulation that in general does not account for thermal and memory effects in the standard Markov approximation.^{20,21}

Calculating the time derivative of $G_{ij\sigma}^<(t, t)$ we arrive at

$$i \frac{\partial}{\partial t} \mathbf{G}_\sigma^<(t, t) = \mathbf{M}_\sigma(t) \mathbf{G}_\sigma^<(t, t) - \Phi_\sigma(t), \quad (6)$$

where the lesser Green function is written in a vector-like form $\mathbf{G}_\sigma^< = [G_{11\sigma}^<, G_{12\sigma}^<, G_{21\sigma}^<, G_{22\sigma}^<]^T$ and $\Phi_\sigma = [\Phi_{11\sigma}^<, \Phi_{12\sigma}^<, \Phi_{21\sigma}^<, \Phi_{22\sigma}^<]^T$. Here $\Phi_{ij\sigma}^<(t) = \Phi_{ij\sigma}^r(t) - \Phi_{ij\sigma}^a(t)$, with

$$\Phi_{ij\sigma}^r(t) = \int_{-\infty}^t dt_1 G_{ij\sigma}^r(t, t_1) \phi_{j\sigma}(t_1, t), \quad (7)$$

and

$$\Phi_{ij}^a(t) = \int_{-\infty}^t dt_1 \phi_{i\sigma}(t, t_1) G_{ij\sigma}^a(t_1, t). \quad (8)$$

The matrix in Eq. (6) is given by

$$\mathbf{M}_\sigma(t) = \begin{bmatrix} -i\Gamma_{1\sigma} & -\gamma e^{-i\omega t} & \gamma e^{i\omega t} & 0 \\ -\gamma e^{i\omega t} & \omega_{12} - \frac{i}{2}\Gamma_\sigma & 0 & \gamma e^{i\omega t} \\ \gamma e^{-i\omega t} & 0 & \omega_{21} - \frac{i}{2}\Gamma_\sigma & -\gamma e^{-i\omega t} \\ 0 & \gamma e^{-i\omega t} & -\gamma e^{i\omega t} & -i\Gamma_{2\sigma} \end{bmatrix}, \quad (9)$$

with $\omega_{ij} = \epsilon_i - \epsilon_j$ and $\Gamma_\sigma = \Gamma_{1\sigma} + \Gamma_{2\sigma}$. It is yet valid to note that in the absence of the reservoirs, Eq. (6) reduces to the well known semiconductor Bloch equations.² In order to determine $\Phi_\sigma(t)$ we need the retarded and advanced Green functions $G_{ij}^{r,a}(t, t')$. Taking the time derivative with respect to t' we obtain

$$-i \frac{\partial}{\partial t'} \mathbf{G}_\sigma^r(t, t') = \delta(t - t') \begin{bmatrix} \chi_+ \\ \chi_- \end{bmatrix} + \mathbf{P}_\sigma(t') \mathbf{G}_\sigma^r(t, t'), \quad (10)$$

where $\mathbf{G}_\sigma^r = [G_{11\sigma}^r, G_{12\sigma}^r, G_{21\sigma}^r, G_{22\sigma}^r]^T$, χ_+ and χ_- are the two-component Pauli spinors, $\chi_+ = [1, 0]^T$ and $\chi_- = [0, 1]^T$, and the matrix $\mathbf{P}_\sigma(t')$ is defined according to

$$\mathbf{P}_\sigma(t) = \begin{bmatrix} \delta_1 & \gamma e^{-i\omega t'} & 0 & 0 \\ \gamma e^{i\omega t'} & \delta_2 & 0 & 0 \\ 0 & 0 & \delta_1 & \gamma e^{-i\omega t'} \\ 0 & 0 & \gamma e^{i\omega t'} & \delta_2 \end{bmatrix}, \quad (11)$$

with $\delta_l = \epsilon_l - \frac{i}{2}\Gamma_{l\sigma}$. Solving numerically Eqs. (6) and (10) we obtain the occupation $n_{i\sigma}(t)$ and the photocurrent. In what follows we present our results.

III. PARAMETERS

In order to keep the generality of our results, we express the time in units of $t_0 = \hbar/\Gamma_0$, where Γ_0 is proportional to the tunneling rate between dot and reservoirs. For simplicity we assume the wideband limit, where the tunneling rates are energy independent and we set $\Gamma_{1\sigma} = \Gamma_{2\sigma} = \Gamma_0$. The current unit is given by $I_0 = e\Gamma_0/\hbar$ and all energies are in units of Γ_0 .²² Experimentally, Γ_0 depends on the tunnel barrier and it can be easily controlled by an external gate voltage. We find for quantum dot systems $\Gamma_0 \sim 1\mu\text{eV} - 100\mu\text{eV}$,²³⁻²⁵ which results in $I_0 \sim 0.24n\text{A} - 24n\text{A}$.²⁶ The time t_0 ranges in the interval $t_0 \sim 6.5\text{ps}$ ($\Gamma_0 = 100\mu\text{eV}$) - 0.65ns ($\Gamma_0 = 1\mu\text{eV}$).²⁷ Additionally, the quantum dot valence and conduction band levels are given by $\epsilon_{1\sigma} = \epsilon_1 = -100\Gamma_0$ and $\epsilon_{2\sigma} = \epsilon_2 = 2\Gamma_0$, respectively.²⁸ Both levels are measured with respect to the chemical potential $\mu_2 = 0$, which is taken as our energy reference. The chemical potential of the right side μ_1 is given by $\mu_1 - \mu_2 = eV_b$, where V_b is the bias voltage. In what follows we adopt $eV_b = 10\Gamma_0$. Finally, we assume $k_B T \sim 0.1\Gamma_0 - 2\Gamma_0$ and $\gamma = 7\Gamma_0$,²⁹ except when those parameters explicitly change in the plots.

IV. RESULTS

Figure 2(a)-(b) shows the evolution of the electron and hole occupations in the quantum dot for differing temperatures $k_B T$. At $t = 0$ the valence band level is fully occupied with $n_1 = 1$ while the occupation of the conduction band is $n_2 \approx 0.1$.³⁰ This small occupation comes from the proximity of the level ϵ_2 to the Fermi energy of the left reservoir, which allows thermal excited electrons to tunnel into the dot. Initially ($t = 0$) the quantum dot occupation is calculated using the equation

$$n_{i\sigma}(t = 0) = \int \frac{d\epsilon}{2\pi i} G_{ii\sigma}^<(\epsilon), \quad (12)$$

where the lesser Green function is given by the Keldysh equation $G_{ii\sigma}^<(\epsilon) = G_{ii\sigma}^r(\epsilon) \Sigma_{i\sigma}^<(\epsilon) G_{ii\sigma}^a(\epsilon)$, where $G_{ii\sigma}^{r(a)}$ is the retarded (advanced) Green function of the dot attached to the leads without laser field and $\Sigma_{i\sigma}^< = i\Gamma_{i\sigma} f_i$. As $k_B T$ increases, electrons in the left electrode acquire enough thermal energy to enhance the population n_2 at $t = 0$, while n_1 remains the same due to $\epsilon_1 \ll \epsilon_F$. When the system starts to evolve in the presence of a laser field, the occupations n_1 and n_2 develop the characteristic Rabi oscillations. In the small temperature regime these oscillations are more pronounced for small times and become suppressed as the time increases. This is due to the decoherence imposed by the tunneling between dot and reservoirs. For large enough times both n_1 and n_2 reach constant values.

As the temperature increases, the amplitude of the Rabi oscillations shrinks for all times. This is directly related to the enhancement of the initial population n_2 with temperature. With the level ϵ_2 becoming more populated, the Pauli exclusion principle makes it more difficult to one electron with the same spin in the valence band (ϵ_1) to jump to the conduction band (ϵ_2). So we observe two sources of suppression to the coherent Rabi oscillations: (i) coupling to reservoirs and (ii) thermal activated Pauli blockade.

The photocurrent seen in Fig. 2(c), at least to some extent, reflects the n_2 behavior. It oscillates in time with a decreasing amplitude, tending to a stationary nonzero value. Additionally, the amplitude of the Rabi oscillations is also reduced as $k_B T$ increases, following the behavior of n_2 . Interestingly, for small enough temperatures and shorter times, the photocurrent oscillations attain negative values, which corresponds to an unusual flow of electrons from the reservoir into the dot (see solid line, $k_B T = 0.1\Gamma_0$, around $t = 0.5t_0$). In order to gain further insight of this effect, in the inset of Fig. 2(c) we show separately the current components I_{out} and I_{in} . The outgoing current is positive which means that electrons are flowing from the dot to the reservoir. The incoming current gives a negative contribution to the current, which corresponds to electrons flowing in the opposite way, i.e., from the electrode into the dot. Around $t = 0.5t_0$, the I_{in} component presents a dip, which pulls down the total photocurrent, making it negative. When

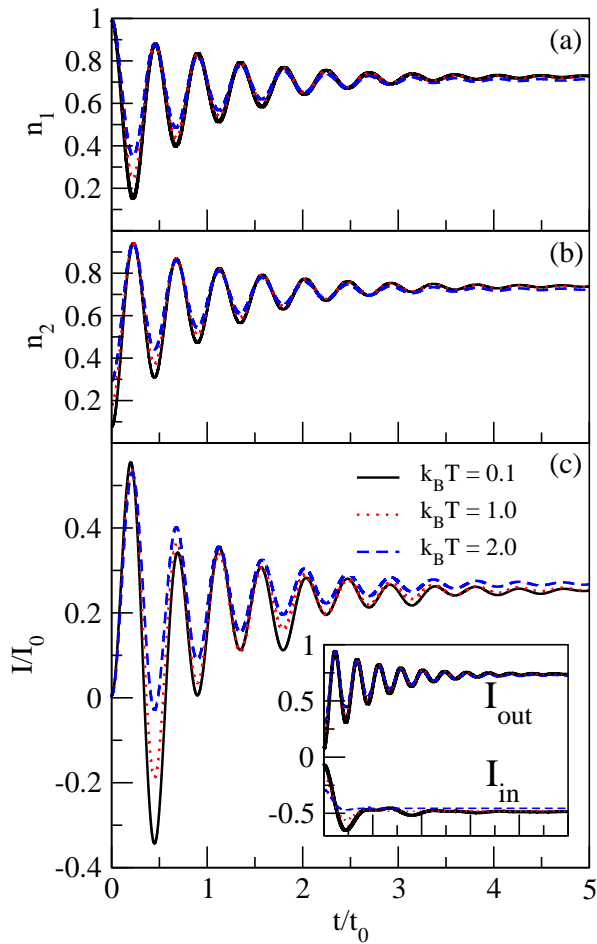


FIG. 2. (Color online)(a)-(b) Occupation of the levels ϵ_1 and ϵ_2 and (c) photocurrent as a function of time for differing temperatures. As time evolves all these quantities exhibit coherent Rabi oscillations. The amplitude decreases with time due to the incoherent tunneling between dot and electrodes. The oscillation amplitude is also suppressed as $k_B T$ increases due to a thermal induced Pauli blockade. For $t \approx 0.5t_0$ the photocurrent is dominated by a backwards current, thus becoming negative. In the inset we show separately the in and out current components.

$k_B T$ increases, this dip is suppressed and the photocurrent assumes positive values for all times.

Figure 3(a) shows how n_1 and n_2 evolves as a function of the parameter γ , for differing temperatures. For all $k_B T$ values we observe $n_1 = 1$ for $\gamma = 0$, while n_2 increases with $k_B T$ for $\gamma = 0$. This enhancement of n_2 with temperature comes from the thermal excited electrons in the reservoir that acquires enough energy to jump into the dot as $k_B T$ increases. Both n_1 and n_2 are obtained via Eq. (12) for $\gamma = 0$. In the presence of the laser field, n_2 increases monotonically with γ , while n_1 is initially suppressed and then it is enhanced, thus developing a minimum around $\gamma \approx \epsilon_2 - \mu_2 = 2\Gamma_0$. Note also that n_2 presents a further enhancement near $\gamma = 2\Gamma_0$. In the inset of Fig. 3(a) we show the sum $n = n_1 + n_2$ against γ .

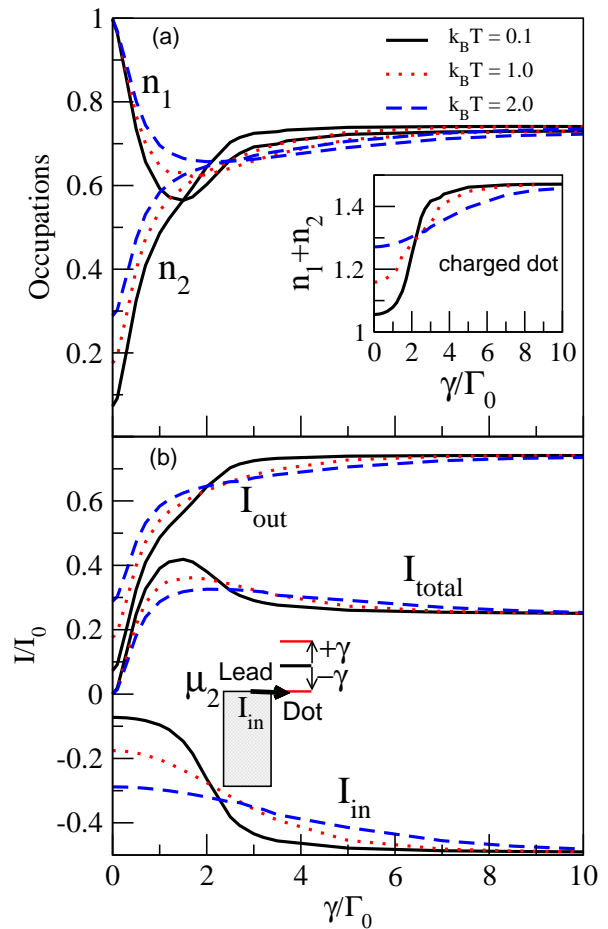


FIG. 3. (Color online)(a) Occupations n_1 and n_2 and (b) current components against γ . While n_2 increases monotonically with γ , n_1 is initially suppressed, reaches a minimum and then increases slightly. Oppositely, the photocurrent increases with γ , reaches a maximum and then becomes slightly suppressed. This nonmonotonic behavior in both n_1 and I can be understood looking at the current component I_{in} . When $\gamma \approx \epsilon_2 - \mu_2 = 2\Gamma_0$, electrons in the reservoir can tunnel into the dot, thus populating ϵ_2 . This enhancement (in modulus) of the backwards current suppresses the photocurrent for $\gamma > 2\Gamma_0$ and increases further n_2 . In the inset we plot $n_1 + n_2$. Note that the dot charges for $\gamma > 2\Gamma_0$.

When the resonant condition $\gamma = \epsilon_2 - \mu_2$ is attained, the total occupation presents a steeper enhancement for low temperature. For larger $k_B T$ a more broadened increasing is found. It is valid to note that the sum $n_1 + n_2$ is not limited to one, as expected in a standard two-level system with one level being initially occupied and the other one being initially empty. Here the level ϵ_2 is not populated only by the laser field, but also by the left reservoir. The occupation profiles will be more clearly understood looking at the current components in the next plot.

In Fig. 3(b) we plot separately the current components I_{out} , I_{in} and the total current $I = I_{out} + I_{in}$. While the outgoing current follows n_2 , the incoming current is strongly increased (in modulus) around $\gamma \approx \epsilon_2 - \mu_2$.

As a result, the photocurrent is suppressed due to this backwards current, thus developing a peak close to $\gamma = \epsilon_2 - \mu_2$. Increasing even further the temperature, the thermal fluctuations of the reservoirs yield to a more effective injection of electrons into the dot. This makes I_{in} starts at higher absolute values for $\gamma \lesssim 2\Gamma_0$. This amplification of I_{in} suppresses the photocurrent when compared to its low temperature profile. In the presence of a laser field in resonance with the difference $\epsilon_2 - \epsilon_1$, doublets emerge in the spectrum of the system,^{31,32} as illustrated in the drawn of Fig. 3(b).³³ As the laser intensity increases, the lower energy peak of the doublet eventually attain resonance with the reservoir chemical potential at $\gamma = \epsilon_2 - \mu_2$. This allows electrons to resonantly tunnel from the lead into the dot, thus generating a backwards current that suppresses the total photocurrent and increases the n_2 population. When the lower peak lies below μ_2 , the enhancement of $k_B T$ tends to depopulate this channel, consequently suppressing I_{in} , as seen in Fig. 3(b) for $\gamma \gtrsim 2\Gamma_0$.

Finally, it is valid to point out that the I_{in} current component plays a role in the transport whenever $\epsilon_2 - \gamma \leq \mu_2$, which allows electrons in the reservoir to resonant tunnel to the dot. It is possible to entirely suppress the incoming current by moving ϵ_2 high enough above μ_2 , so that $\epsilon_2 - \gamma > \mu_2$. For this regime electrons can flow only in one direction, i.e., from the dot to the reservoir, thus reducing the backwards charge flow. Fig. 4 shows the photocurrent against time for different ϵ_2 values. For $\epsilon_2 = 2\Gamma_0$ and $5\Gamma_0$ the channel $\epsilon_2 - \gamma$ lies below μ_2 , as illustrated in the energy diagram at the lower part of the panel. This results in a relatively high $|I_{in}|$ component (see the inset). On the contrary, for $\epsilon_2 = 10\Gamma_0$ and $20\Gamma_0$ we find $\epsilon_2 - \gamma$ higher than μ_2 (see the upper energy diagram sketched), which suppresses $|I_{in}|$ and makes the total current larger.

V. CONCLUSION

In conclusion, via nonequilibrium Green function technique we have investigated the dynamics of electron-hole pairs in a quantum dot tunnel coupled to Fermionic reservoirs. We found that the thermal fluctuation of the reservoir and consequent occupation of the conduction band level appears as a new source of decoherence for the opti-

cally induced Rabi oscillation in QDs, which has not been reported yet. As temperature increases, the thermal excited carriers in the left reservoir acquires enough energy to tunnel into the dot. This gives rise to an enhancement of electronic dot population, which results in a thermal activated Pauli blockade that suppresses slightly the Rabi oscillations. This effect is strongly dependent on the temperature of the reservoirs and on the mismatch between ϵ_2 and μ_2 . Finally, a nonlinearity signature is found in the current against γ . This results from a doublet that brings into resonance a transport channel with the chemical potential μ_2 . This laser induced resonance generates

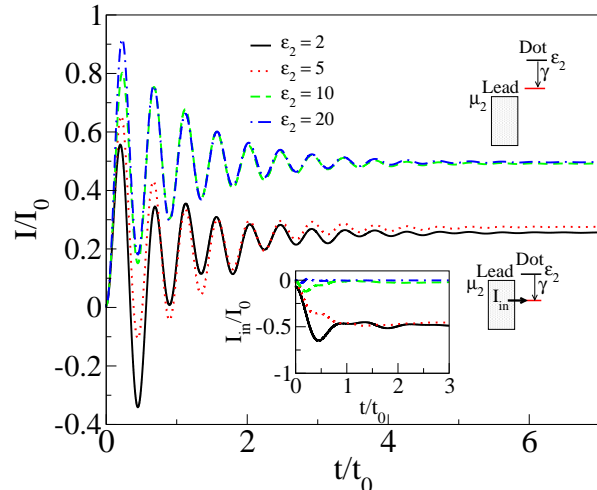


FIG. 4. (Color online) Photocurrent against time for different ϵ_2 values, with respect to μ_2 . As ϵ_2 increases the photocurrent is amplified. This is due to the suppression of the incoming current for larger ϵ_2 . The temperature adopted is $k_B T = 0.1\Gamma_0$. In the inset we show the incoming current component for all the ϵ_2 values used. As ϵ_2 enlarges, the incoming current tends to zero.

a competition between outgoing and incoming currents in the quantum dot that yields to the observed nonlinearities. As a final remark, we note that the present study is a fundamental example of the use of nonequilibrium Green function for optical processes, which can be applied to more intricate systems, including non-Markovian processes.

The authors acknowledge the Brazilian agencies CNPq, CAPES and FAPEMIG for financial support.

¹ Quantum Transport: Atom To Transistor, S. Datta, Cambridge University Press (2005).

² H. Haug and A. P. Jauho, Quantum Kinetics in Transport and Optics of Semiconductors, Second Edition, Springer Solid-State Sciences **123** (2008).

³ T. E. Rosson, S. M. Claiborne, J. R. McBride, B. S. Stratton, S. J. Rosenthal, Journal of the American Chemical Society (2012).

⁴ H. N. S. Krishnamoorthy, Z. Jacob, E. Narimanov, I. Kretzschmar, V. M. Menon, Science **336**, 6078 (2012).

⁵ T. H. Stievater, X. Li, D. G. Steel, D. Gammon, D. S. Katzer, D. Park, C. Piermarocchi, and L. J. Sham, Phys. Rev. Lett. **87**, 133603 (2001).

⁶ H. Kamada, H. Gotoh, J. Temmyo, T. Takagahara, and H. Ando, Phys. Rev. Lett. **87**, 246401 (2001).

⁷ P. Borri, W. Langbein, S. Schneider, U. Woggon, R. L.

- Sellin, D. Ouyang, and D. Bimberg, Phys. Rev. B **66** 081306 (2002).
- ⁸ S. Michaelis de Vasconcellos, S. Gordon, M. Bichler, T. Meier, and A. Zrenner, Nature **4**, 545 (2010).
- ⁹ D. R. McCamey, H. A. Seipel, S.-Y. Paik, M. J. Walter, N. J. Borys, J. M. Lupton, and C. Boehme, Nature Mater. **7**, 723 (2008).
- ¹⁰ M. E. Flatté, J. M. Byers, and W. H. Lau, Semiconductor Spintronics and Quantum Computation, Edited by D. D. Awschalom, D. Loss, and N. Samarth (Springer, New York, 2002).
- ¹¹ A. Greilich, S. G. Carter, D. Kim, A. S. Bracker, and D. Gammon, Nature Photon. **5**, 702 (2011).
- ¹² A. Zrenner, E. Beham, S. Stuffer, F. Findeis, M. Bichler, and G. Abstreiter, Nature **418**, 612 (2002).
- ¹³ J. M. Villas-Bôas, S. E. Ulloa, and A. O. Govorov, Phys. Rev. B **75**, 155334 (2007).
- ¹⁴ H. S. Borges, L. Sanz, J. M. Villas-Bôas, and A. M. Alcalde, Phys. Rev. B **81** 075322 (2010).
- ¹⁵ A. J. Ramsay, A. V. Gopal, E. M. Gauger, A. Nazir, B. W. Lovett, A. M. Fox, and M. S. Skolnick, Phys. Rev. Lett. **104**, 017402 (2010).
- ¹⁶ A. J. Ramsay, T. M. Godden, S. J. Boyle, E. M. Gauger, A. Nazir, B. W. Lovett, A. M. Fox, and M. S. Skolnick, Phys. Rev. Lett. **105**, 177402 (2010).
- ¹⁷ P. W. Fry, I. E. Itskevich, S. R. Parnell, J. J. Finley, L. R. Wilson, K. L. Schumacher, D. J. Mowbray, M. S. Skolnick, M. Al-Khafaji, A. G. Cullis, M. Hopkinson, J. C. Clark, and G. Hill, Phys. Rev. B **62**, 16784 (2000).
- ¹⁸ Here the level in the valence band ($i = 1$) of the quantum dot couples only to the right lead ($i = 1$), while the conduction band level ($i = 2$) couples only to the left lead ($i = 2$).
- ¹⁹ F. M. Souza, J. C. Egues, and A. P. Jauho, Braz. J. Phys. **34**, 565 (2004).
- ²⁰ J. M. Villas-Bôas, S. E. Ulloa, and A. O. Govorov, Phys. Rev. Lett. **94**, 057404 (2005).
- ²¹ For a non-Markovian description see D. Mogilevtsev, A. P. Nisovtsev, S. Kilin, S. B. Cavalcanti, H. S. Brandi, and L. E. Oliveira, Phys. Rev. Lett. **100**, 017401 (2008).
- ²² The parameter Γ_0 in our model gives the relaxation rate due to incoherent tunneling processes. The characteristic relaxation time is \hbar/Γ_0 .
- ²³ D. G.-Gordon, H. Shtrikman, D. Mahalu, D. A.-Magder, U. Meirav, M. A. Kastner, Nature **391**, 156 (1998).
- ²⁴ D. Goldhaber-Gordon, J. Göres, M. A. Kastner, H. Shtrikman, D. Mahalu, and U. Meirav, Phys. Rev. Lett. **81**, 5225 (1998).
- ²⁵ F. Simmel, R. H. Blick, J. P. Kotthaus, W. Wegscheider, and M. Bichler, Phys. Rev. Lett. **83**, 804 (1999).
- ²⁶ It is valid to point out that one can control the noise levels in nanoscale conductors in the presence of ac-fields, by tuning the amplitude of the field, see for instance, S. Camalet, J. Lehmann, S. Kohler, and P. Hänggi, Phys. Rev. Lett. **90**, 210602 (2003).
- ²⁷ The state of the art quantum transport experiments allow ultrafast pA-photocurrent measurement in the ps time scale. For instance, it was recently measured ultrafast photocurrent dynamics in a p - i - n carbon nanotube based junction, see N. M. Gabor *et al.*, Phys. Rev. Lett. **108**, 087404 (2012).
- ²⁸ The parameter $\epsilon_{1\sigma} = -100\Gamma_0$ is in fact much smaller than the realistic values for semiconductor dots that result in excitonic energy typically of $\epsilon_2 - \epsilon_1 \approx 1\text{eV}$. However, since $\epsilon_{1\sigma}$ is already much larger than any other energy scale in the problem, if its value is increased even further no changes will be observed in the results.
- ²⁹ It is valid to note that our formulation wouldn't be valid in the limit where γ is comparable to the difference $\epsilon_2 - \epsilon_1$ or the laser frequency ω , since we adopt the rotating wave approximation. Additionally, in the experimental point of view γ is much smaller than $\epsilon_2 - \epsilon_1$ or ω .
- ³⁰ It is valid to point out that in the standard approach of the two-level semiconductor quantum dot systems, based on density matrix formalism, it is adopted the base $|0\rangle$ and $|1\rangle$ for no-exciton and one-exciton in the dot, respectively. The initial state $|0\rangle$ in our formalism stands to $n_1 = 1.0$ and $n_2 = 0.0$, which means that the conduction band is empty, while the valence band is filled with one electron. Though, due to the thermal effects reported here, the occupation n_2 fluctuates, thus resulting in $n_2 \neq 0$.
- ³¹ S. H. Autler and C. H. Townes, Phys. Rev. **100**, 703 (1955).
- ³² B. R. Mollow, Phys. Rev. **188**, 1969 (1969).
- ³³ A similar pair of doublets in a two-level system also takes place when, instead of light, a phonon field connects the levels. See, for instance, E. Vernek, E. V. Anda, S. E. Ulloa, and N. Sandler, Phys. Rev. B **76**, 75320 (2007).